Geological Society, London, Special Publications Online First

Cross-strike structures controlling magmatism emplacement in a flat-slab setting (Precordillera, Central Andes of Argentina)

S. Oriolo, M. S. Japas, E. O. Cristallini and M. Giménez

Geological Society, London, Special Publications, first published November 21, 2013; doi 10.1144/SP394.6

Cross-strike structures controlling magmatism emplacement in a flat-slab setting (Precordillera, Central Andes of Argentina)

S. ORIOLO[1]*, M. S. JAPAS[2], E. O. CRISTALLINI[3] & M. GIMÉNEZ[4]

[1]*Departamento de Ciencias Geológicas, Universidad de Buenos Aires, Intendente Güiraldes 2160, Buenos Aires, Argentina*

[2]*Instituto de Geociencias Básicas, Aplicadas y Ambientales (CONICET-UBA), Intendente Güiraldes 2160, Buenos Aires, Argentina*

[3]*Laboratorio de Modelado Geológico, IDEAN (UBA-CONICET), Intendente Güiraldes 2160, Buenos Aires, Argentina*

[4]*Instituto Geofísico Sismológico Volponi, FCEN, Universidad Nacional de San Juan, Av. José Ignacio de la Roza y Meglioli S/N, San Juan, Argentina*

**Corresponding author (e-mail: seba.oriolo@gmail.com)*

Abstract: Detailed structural, kinematic and geophysical data on the foreland of the Pampean flat-slab segment (Hualilán area, Andean Precordillera of Argentina) have shown that cross-strike structures have had an important role in the evolution of this Andean segment since Miocene times. These structures represent pre-existing crustal fabrics reactivated during the Andean orogeny and could have controlled the emplacement of the Miocene arc-magmatism migrating into foreland due to the flattening of the slab. Likewise, kinematic results obtained for these structures support a similar stress frame to that obtained elsewhere in the Precordillera but showing different motions as a consequence of their high obliquity to the orogen trend. Moreover, they record a reorientation of kinematic axes during Late Miocene–Pliocene times.

Cross-strike structures are steeply dipping cross-strike structural discontinuities represented by wide zones of brittle–ductile deformation (Wheeler 1980; Twiss & Moore 1992; Mueller & Talling 1997). Usually, they represent reactivated pre-existing structures inherited from earlier tectonic phases. They are considered important structures since they can behave either as barriers for seismic ruptures of major faults or as transfer structures linking two adjacent segments of the same fault system (Wheeler 1980; Hudnut *et al.* 1989; Pizzi & Galadini 2009). Likewise, cross-faults cutting across main faults resulted in the formation of fault blocks and therefore could have relevant economic significance (Johnson *et al.* 2002; Saha *et al.* 2006). In some orogenic systems, cross-faults act as channels for crustal fluids and highlight basement-involved deformation. Studies of these faults have renewed discussion about thin-skinned v. thick-skinned tectonics. Hence, the true amount of orogenic shortening when cross-faults are present has to be carefully considered (Tavarnelli *et al.* 2004).

The Central Andes display two flat-slab sectors, the Peruvian (5–15°S) and the Pampean (28–33°S) segments (Ramos *et al.* 2002), which resulted from the subduction of the Nazca and Juan Fernández aseismic ridges, respectively (Pilger 1981; Gutscher *et al.* 2000). Linked to the subduction of the Nazca Plate under the overriding South American Plate, the Central Andes (5–47°S; Gansser 1973) show oblique structures compartmentalizing the orogen, and controlling its architecture (Baldis & Vaca 1985; Salfity 1985) as well as its kinematic evolution (Rossello *et al.* 1996; Urreiztieta 1996; Ré *et al.* 2001; Japas & Ré 2005, 2012). Both flat-slab regions show similar tectonic features such as arc-related magmatism and compressional/transpressional deformation migrating more than 600 km inland from the trench. Although inland migration of arc-magmatism and deformation has been much described along these segments, studies concerning the structural control of the former are scarce. Hence, the Central Andes between 28° and 33°S provide an excellent opportunity to study the evolution of an active margin linked to flat-slab subduction and, particularly, the Precordillera offers the chance to analyse the relationship between inland migration of deformation and magmatism.

References about cross-strike structures in the Pampean flat-slab segment are still scarce. Within this framework, contributions from Baldis & Vaca (1985), Japas (1998), Ré *et al.* (2000, 2001), Japas *et al.* (2002*a*, *b*) and Ré & Japas (2004) stand out. These latter authors (Japas 1998; Ré *et al.* 2000,

From: Llana-Fúnez, S., Marcos, A. & Bastida, F. (eds) *Deformation Structures and Processes within the Continental Crust*. Geological Society, London, Special Publications, **394**, http://dx.doi.org/10.1144/SP394.6

2001; Japas *et al.* 2000*a*, *b*; Ré & Japas 2004) have recognized two systems of conjugated brittle–ductile megashear zones in the Precordillera: NNW left-lateral and NNE right-lateral transpressional structures, and WNW left-lateral and ENE right-lateral transtensional ones. The former consist of gently oblique zones whereas the latter comprise cross-strike structures. Contributions on the relationship between cross-strike structures and magmatism in the flat-slab segment are restricted to the Sierras Pampeanas, particularly to the Sierra de San Luis (Urbina *et al.* 1995, 1997; Sruoga *et al.* 1996; Sruoga & Urbina 2008; Urbina & Sruoga 2009; Japas *et al.* 2010, 2011*a*, *b*). However, many authors have outlined the importance of the structural control of magmatism. De Saint Blanquat & Tikoff (1997), de Saint Blanquat *et al.* (1998), Brown & Solar (1999), Žák *et al.* (2005), Lara *et al.* (2006) and Romeo *et al.* (2006) have remarked on the interaction between transpression/transtension and magmatism. Recently, Acocella & Funiciello (2010) have provided a detailed study of many arcs and their kinematic and structural settings, concluding that regional or local extension is always required for volcanic output.

The aim of this paper is to contribute to the understanding of the development and kinematics of cross-strike structures as well as their interaction with magmatism in a flat-slab setting. The integration of tectonic fabric analysis and structural, kinematic and magnetometric data have provided information that helps to constrain temporal and spatial relationships between magmatism and deformation.

Geological setting

The main morphostructural units in the Pampean flat-slab segment in Argentina are the Frontal Cordillera, the Precordillera and the Sierras Pampeanas (Fig. 1a). The Frontal Cordillera represents a basement block made up mostly of Palaeozoic sedimentary rocks intruded by Permo-Triassic and Jurassic granitoids uplifted during the Andean orogeny (Heredia *et al.* 2002). The Precordillera comprises a NNE-trending range that represents a foreland composite fold-and-thrust belt and can be divided into three main morphostructural units: Western, Central and Eastern Precordillera (Fig. 1b). Western and Central Precordillera show east-verging epidermic deformation while the Eastern Precordillera represents a west-verging thick-skinned fold-and-thrust belt (Allmendinger *et al.* 1990; Cristallini & Ramos 2000). The Sierras Pampeanas represent a series of uplifted blocks constituted mostly of metamorphic and igneous rocks of Neoproterozoic to Palaeozoic ages.

The study area is located in Hualilán in the Central Precordillera of San Juan, Argentina (Fig. 1b). This region includes an intermontane basin known as the Pampa de Hualilán that is bounded by several ranges (Fig. 2). The locality is of special interest because of the presence of outcrops of Miocene dacites that represent one of the very few manifestations of the Miocene arc migration into the foreland due to the flat-slab process in the Precordillera (Kay & Abbruzzi 1996). These volcanic and subvolcanic rocks are associated with hydrothermal veins related to the late magmatic stages (Logan 2000). The stratigraphic column also comprises Ordovician siliciclastic rocks (Sierra de la Invernada Formation) and limestones (San Juan Formation), Siluro-Devonian metasedimentary rocks (Tucunuco and Gualilán Groups), Miocene continental sediments (Cuculí Formation), and Quaternary alluvial, aeolian and lacustrine sediments (Fig. 2).

Tectonic fabric analysis

Tectonic fabric of the Precordillera

Tectonic fabric analysis was carried out in the Precordillera and the Hualilán area. In the first case, a chromatic scale was used to discriminate between fabric elements (structural lineaments, traces of fold axes and faults) with different orientations (van Gool & Piazolo 2006; Japas *et al.* 2013) using data already published by Ragona *et al.* (1995). Fabric elements in Hualilán were recognized on the basis of satellite imagery, aerial photographs at 1:25 000 and 1:50 000 scales, and field work.

On a regional scale, the Precordillera fold-and-thrust belt shows a north – NNE trend of major faults and fold axes (Fig. 3a). However, detailed fabric analysis revealed the presence of three domains according to the orientation of their constituent elements (Fig. 3b).

Domain I displays a WNW orientation and is distinguishable in three areas (IA, IB, IC; Fig. 3b). Tectonic fabric elements have mostly a NW–NNW strike but ENE to WNW structural features are also common. It must be emphasized that all Miocene volcanic and subvolcanic rocks crop out within this domain. On the other hand, domain II exhibits a NNE trend and fabric elements with the same orientation, whereas domain III has a NNE orientation and NNW structural features.

Sector IA (Fig. 3b) shows mostly NW to NNW fabric elements and matches the Miocene Northern Precordillera volcanic belt defined by Limarino *et al.* (2002). Sector IB includes many structures striking WNW–ENE and shows a regional WNW distribution of Miocene igneous rocks.

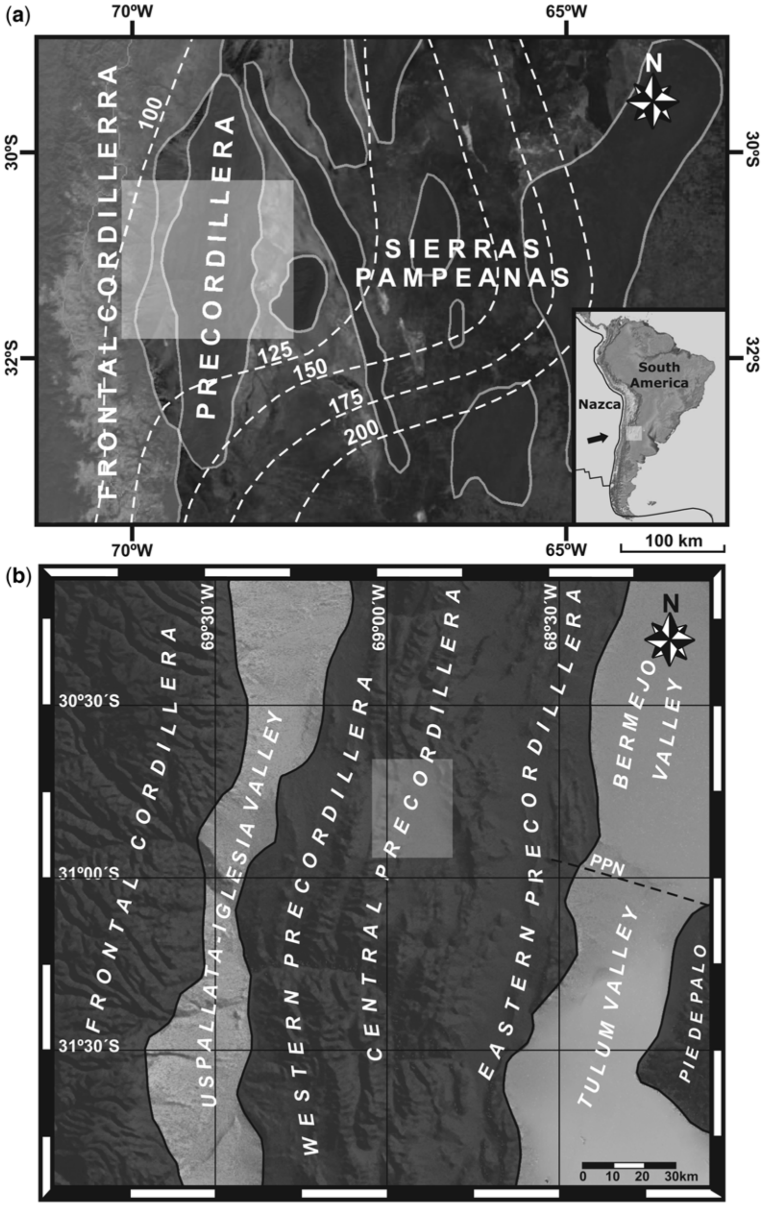

Fig. 1. (**a**) Location of the Andean flat-slab segment in the Central Andes. Contours of depth (km) of oceanic slab after Cahill & Isacks (1992) and the main morphostructural units are shown. Inset indicates the regional Andean subduction and the Pampean flat-slab segment in Argentina. The shaded area is shown in (b). (**b**) Main morphostructural units between 30° and 32°S. The study area is shown by the light-grey rectangle. PPN, Pie de Palo Norte lineament.

These outcrops are mostly located in the Hualilán area and in the Cerro Negro de Iglesia which is placed in the Western Precordillera (Leveratto 1976; Gómez Rivarola 2007). A more complex pattern of deformation is observed in sector IC where NNW structures dominate.

Structure of the Hualilán area

Detailed mapping in the eastern area of sector IB shows the presence of two main structural systems (Fig. 3a). The first system includes NNW to NNE west-dipping thrusts, while the second one

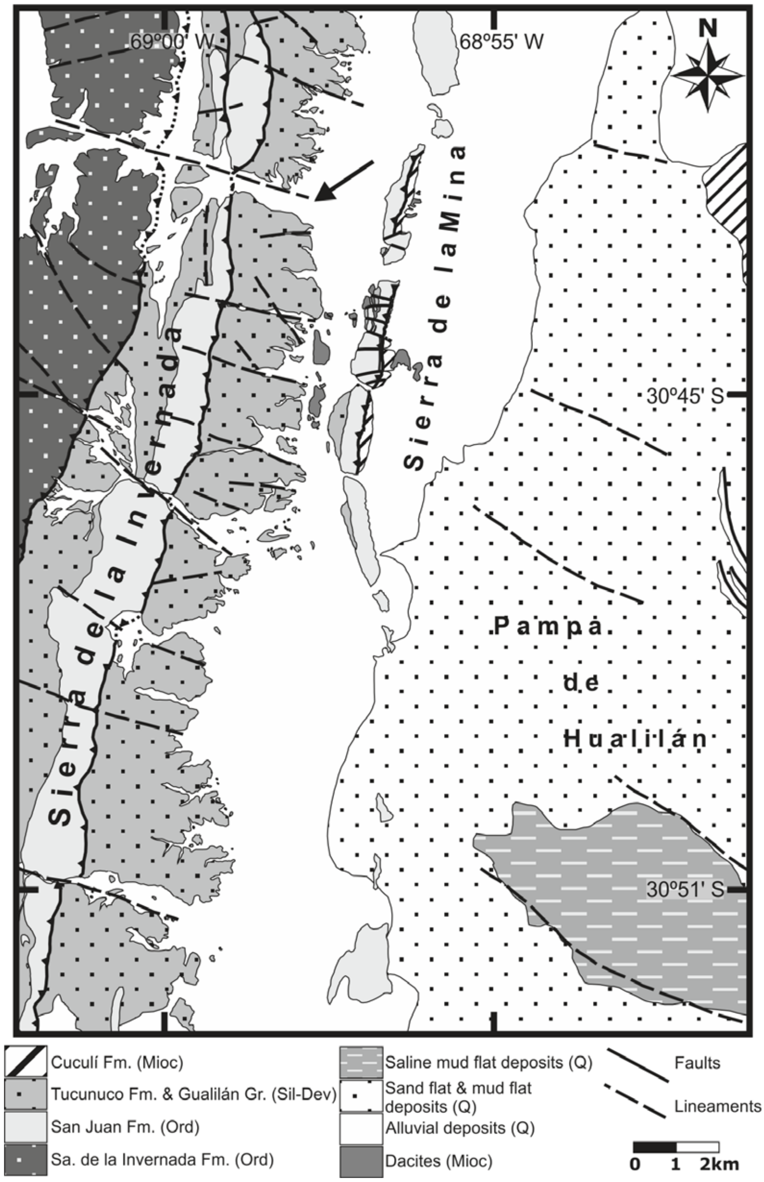

Fig. 2. Geological map of the study area. The black arrow indicates the WNW lineament that cross-cuts the Sierra de la Invernada.

contains WNW to ENE structures with strike-slip displacement.

The Sierra de la Invernada is located between the Western and Central Precordillera and shows a NNE regional trend (Fig. 2). It is made up of Early Palaeozoic units thrusted and folded with NNE and NNW strikes. Many WNW to ENE lineaments are also present, one of which exhibits a WNW strike, and cross-cuts the whole range (Fig. 2).

East of the Sierra de la Invernada (Fig. 2), the Sierra de la Mina is comprised of a west-dipping homoclinal structure with a basal detachment thrust which strikes NNE in the central area, to NNW in the southern and northern ones. Despite its short length, the Sierra de la Mina is of special interest because of the presence of several oblique structures associated with Miocene volcanic rocks. WNW to ENE cross-faults controlled

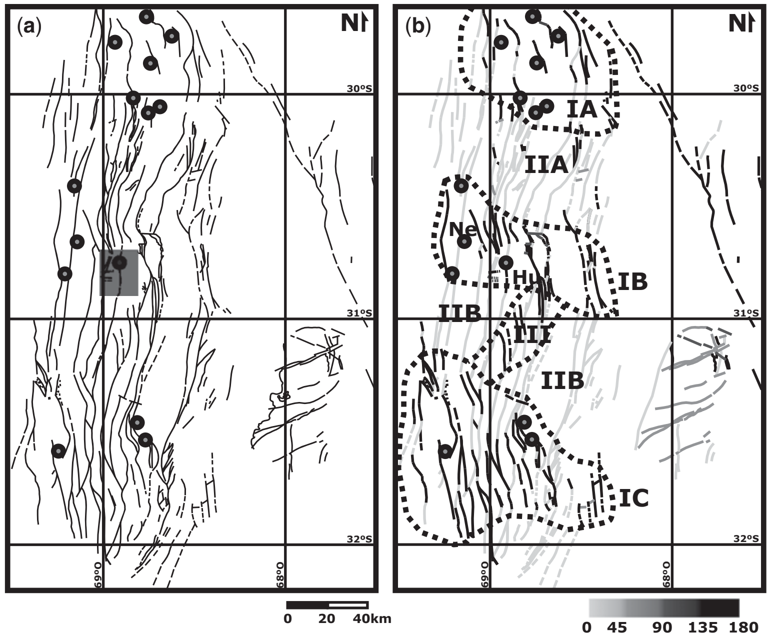

Fig. 3. (**a**) Map of tectonic fabric elements (faults, lineaments and fold axes traces) in the Precordillera and Western Sierras Pampeanas (modified after Ragona *et al.* 1995). Main outcrops of Miocene igneous rocks are represented by grey dots. The shaded area indicates the study area from Figure 2. (**b**) Map from (a) where tectonic fabric elements have been discriminated using a chromatic scale according to their orientation. Different domains (I, II, III) and sectors (A, B, C) recognized from the chromatic analysis are shown, as well as the two main localities with Miocene igneous rocks mentioned in this work (Hu, Hualilán; Ne, Cerro Negro de Iglesia). It is observed that Miocene igneous rock outcrops are restricted to domain I.

the development of the gullies that cross-cut the range. Likewise, neotectonic activity reported by Bastías *et al.* (1984) and Bastías (1985) in the central block of the Sierra de la Mina as well as along-strike changes in geomorphological and structural features suggest strong segmentation of drainage patterns controlled by these cross-strike structures (Fig. 2). They not only separate areas with differences in their drainage networks but they also represent the watershed in the southern margin of the basin (Oriolo 2012 and references therein).

Surveying of brittle–ductile shear zones of centimetre to metre widths affecting the Miocene dacites reveals the presence of a great number of steeply dipping structures (Fig. 4a). A three-modal distribution includes a WNW mean mode with two subordinated NNE and ENE modes (Fig. 4b). Kinematic analysis of these shear zones is presented in the following section.

The cross-strike structures that are frequent in the Precordillera (Fig. 3) are well represented in the Hualilán area, particularly in the Sierra de la Mina (Fig. 4). Mesoscopic brittle–ductile shear zones also support these observations, though the presence of many oblique WNW to ENE cross-structures seems to be verified at regional to local scale in this region.

Kinematic analysis

Measurements of 3D kinematic indicators were made in brittle–ductile shear zones (Fig. 5) (these zones defined in the sense of Ramsay & Huber 1987)) developed in Miocene dacites and their wall-rock following the method described by Japas *et al.* (2008). These structures consist of planar or curviplanar zones of widely distributed deformation that have centrimetre to metre width where mostly *R* (*Riedel*) shears were measured. Scarce tensional fractures have also been measured. Statistical analysis was performed using the Faultkinwin 5.0 software (Marrett & Allmendinger 1990; Allmendinger *et al.* 2012). This analysis led to the definition of three kinematic populations (Fig. 6a–c) on the basis of the clustering of extension axes (Fig. 6d).

Population A shows kinematic axes (*X:147°/09°*, *Y:306°/81°*, *Z:057°/03°*) that reflect NE shortening

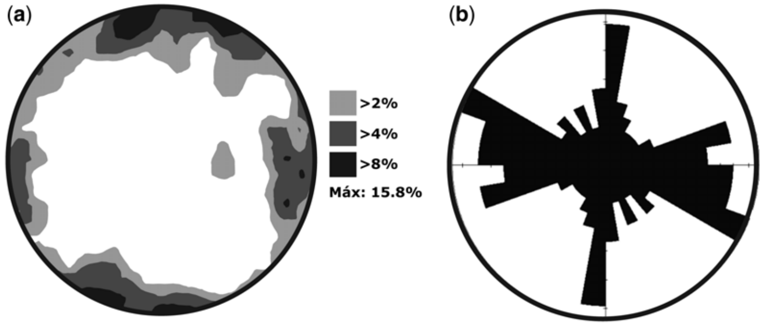

Fig. 4. (**a**) Pole diagram of brittle–ductile shear zones measured in the Hualilán dacites and their wall rock (GEOrient 9.5.0, Holcombe 2011). Equiareal projection, lower hemisphere, $n = 112$. (**b**) Rose diagram showing the WNW mean mode and the two subordinated NNE and ENE modes (frequency intervals of 2%).

related to a dominant strike-slip deformation regime (Fig. 6a). Population B exhibits a similar pattern (*X:206°/03°*, *Y:326°/84°*, *Z:115°/05°*) but reoriented with a WNW shortening direction (Fig. 6b), while in population C (*X:057°/09°*, *Y:290°/74°*, *Z:149°/12°*) *X* and *Z* axes are inverted respect to population A (Fig. 6c).

Mutual cross-cutting relationships suggest that population A predates population B. Both these populations represent local kinematics for the study area during the Andean orogeny and reflect a change from NE to WNW shortening by Late Miocene–Pliocene? times. Results obtained for population C are interpreted as being a consequence of orogenic relaxation.

Shear zones striking WNW and ENE are sinistral strike-slip structures in population A. A minor dominantly normal dip-slip is also present. In population B, both WNW and ENE-striking zones show normal dip-slip with sinistral and dextral strike-slip components, respectively. Likewise, applying criteria from Sanderson & Marchini (1984), low

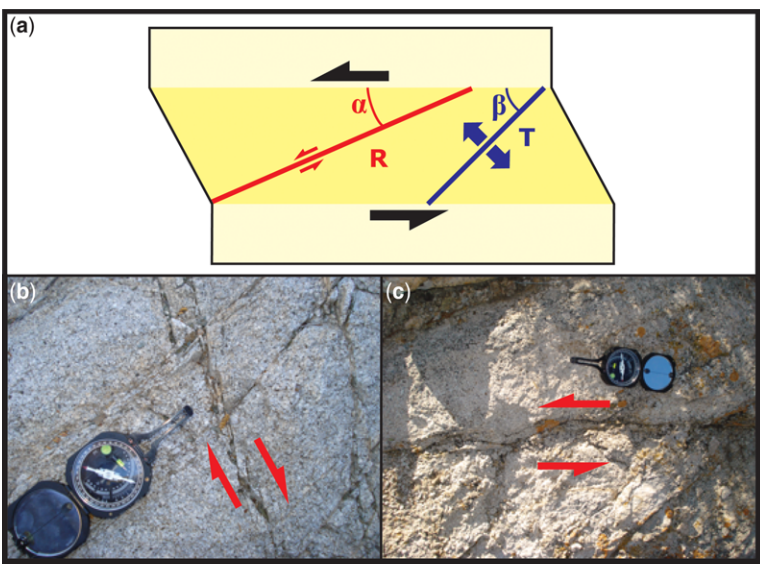

Fig. 5. (**a**) Schematic representation of the brittle–ductile shear zone with Riedel (*R*) shears and tensional fractures (*T*). According to Sanderson & Marchini (1984), $\alpha \approx 20°$ and $\beta \approx 45°$ for strike-slip, whereas both values are lower for transtensional deformation. (**b**) Brittle–ductile shear zone with dextral shearing indicated by *R* shears.
(**c**) Transtensional brittle–ductile shear zone (sinistral shearing) filled with carbonates.

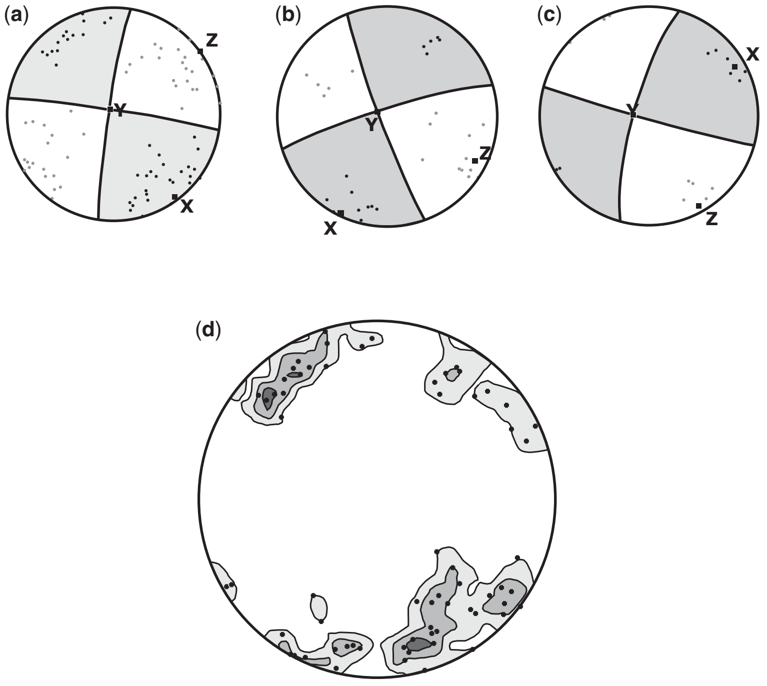

Fig. 6. Kinematic diagrams of extension (black) and shortening (grey) axes obtained using Faultkinwin 5.0 (Marrett & Allmendinger 1990; Allmendinger *et al.* 2012). The main kinematic axes *X*, *Y* and *Z* are represented. (**a**) Population A ($n = 41$). (**b**) Population B ($n = 16$). (**c**) Population C ($n = 8$). (**d**) Extension axes used to define the three different populations ($n = 65$, contour interval 2% per 1% area).

angles between the shear zones and tensional fractures developed within them support transtensional kinematics for cross-strike structures.

Magnetometry

Magnetometric data processing

Aeromagnetometric data were obtained from the Geological Survey (SEGEMAR, Argentina) database. This information was collected at flying heights of 120 m, using north–south lines with spacing of 1000 m and with east–west control lines with spacing of 7500 m. A magnetic anomaly was calculated for the area subtracting the International Geomagnetic Reference Field (IGRF) at the time of the acquisition of the data (Blakely 1995). In order to interprete magnetometric data as the result of geological and structural features, reduction to pole and source parameter imaging (SPI) calculations were made.

Reduction to pole (Baranov 1957) removes the asymmetry caused by the non-vertical magnetization direction so that the anomaly is relocated over the source. The presence of anomalies is interpreted in relation to high-gradient zones over their source. First vertical and horizontal derivatives were calculated over the magnetic anomaly reduced to pole in order to recognize discontinuities that could be compared with structural data.

The SPI method is based on the complex analytical signal theory (Nabighian 1972, 1974, 1984; Roest *et al.* 1992) applied to determine the attributes of the signal. The local wavenumber k is calculated considering the amplitude and phase of the analytical signal, and the algorithm proposed by Blakely & Simpson (1986) led to the calculation of k maximum values. These k values reflect the contacts between different units and the inverse of k is an estimate of the depth of the magnetic source, which is related to high-gradient zones that reflect contacts between different lithologies.

Lithomagnetic domains and lineaments

Lithomagnetic domains were defined on the basis of significant variations in magnetic field parameters, such as intensity and gradient of the field and the geometry of magnetic anomalies. High-gradient zones can be related to the presence of contacts between different units, fractures or faults so that definition of areas of homogeneous magnetic signature led to the recognition of two lithomagnetic units. In this area, the map of the magnetic anomaly reduced to pole (Fig. 7a) reveals a regional variation from NNE to SSW. Magnetization decreases to the SSW with a minimum located at the latitude of the Hualilán swamp. Likewise, many anomalies of high magnetization (>76 nT), short wavelength (1–5 km) and high amplitude (>300 nT) are concentrated in two well-defined areas. The first one is located in the northwestern corner and corresponds to the Cerro Negro de Iglesia area whereas the second cluster is placed in the Hualilán district. Contrasting magnetic properties between Miocene igneous rocks cropping out at both localities and their sedimentary wall rock could satisfactorily explain these anomalies, allowing the recognition of two lithomagnetic domains (Fig. 7b).

Magnetic lineaments were identified on the basis of the horizontal derivative from Figure 7c, though the vertical derivative exhibits a similar pattern (Fig. 7d). Two main groups can be defined according to their orientation (Fig. 7b). The first group consists mainly of NNE lineaments that can be locally oriented in a north to NNW direction. They are continuous along-strike and cross-cut the variation of the regional magnetic field recognized from a NNE to SSW direction (Fig. 7a). In contrast, the second group includes WNW to ENE lineaments, with those of WNW being more frequent. Locally, these oblique lineaments seem to cross-cut the NNE to NNW features.

There is high correlation between the surface structural data described in the section 'Tectonic fabric analysis' and the magnetic lineaments. NNE to NNW lineaments can be interpreted as the result of the main Andean thrusts that made up the Precordillera fold-and-thrust belt while the WNW to ENE lineaments could be related to oblique structures with strike-slip displacement. Those lithomagnetic domains defined as Miocene igneous rocks are located where both sets of oblique lineaments are present. These units are distributed along a major WNW lineament similar to that which cross-cuts the northern Sierra de la Invernada (Fig. 2). A blind thrust, WNW and ENE lineaments and several subsurface igneous bodies can also be recognized below the Holocene deposits in the Pampa de Hualilán (Fig. 2).

Source parameter imaging (SPI)

The map of *k* maximum values and calculated depths is shown in Figure 8. Wide NNE domains of high density *k* values can be observed regionally. However, strong oblique segmentation of these domains also occurs and gives rise to along-strike differences between high and low density areas of *k*.

NNE domains show good correlation with the main NNE to locally NNW lineaments defined by vertical and horizontal derivatives, while the major WNW to ENE lineaments previously defined seem to control the oblique segmentation. It is notable that those lithomagnetic domains representing volcanic and subvolcanic rocks show few *k* maximum values. These results will be discussed in the following section (see *Discussion*).

Estimated depths show values mostly up to 3 km despite the presence of some areas with depths between 3–5 km. Rarely, data from more than 5 km depth are also present. Along-strike differences in depth can be observed in the NNE domains and they could be related to the oblique lineaments. According to the *c.* 15 km depth estimated by Allmendinger *et al.* (1990) and Cristallini & Ramos (2000) for the detachment level of the Precordillera fold-and-thrust belt, results obtained here with the SPI method suggest that structures recognized in the Hualilán area could be developed within a pre-Miocene basement.

Discussion

Relationship between cross-strike structures and Miocene magmatism

Studies related to cross-strike structural discontinuities have mostly focused on their role as barriers that halt major fault segments and fault propagation during seismic rupture (Pizzi & Galadini 2009; Lin *et al.* 2011). However, their relationship with magmatism has been poorly constrained (Pohn 2000; Tavarnelli *et al.* 2004).

Despite the scarcity of detailed works referring to structural controls on Miocene magmatism in the Andean flat-slab segment, many authors have already mentioned the role of WNW to NW structures during Cenozoic localization of magmatism in other regions of the Central Andes. This relationship has been probed in the Puna by Ré *et al.* (2001), Riller *et al.* (2001), Chernicoff *et al.* (2002) and Petrinovic *et al.* (2005, 2010). Contributions from Urbina *et al.* (1995, 1997), Sruoga *et al.* (1996), Sruoga & Urbina (2008), Urbina & Sruoga (2009) and Japas *et al.* (2010, 2011*a*, *b*) have demonstrated the link between a WNW to NW transtensional belt and the emplacement of Miocene–Pliocene magmatic arc rocks (Tertiary Volcanic Belt of San Luis) during the migration of magmatism associated with the Pampean flat-slab in the Sierras Pampeanas foreland.

Regional tectonic fabric analysis within the Precordillera suggests the presence of WNW to

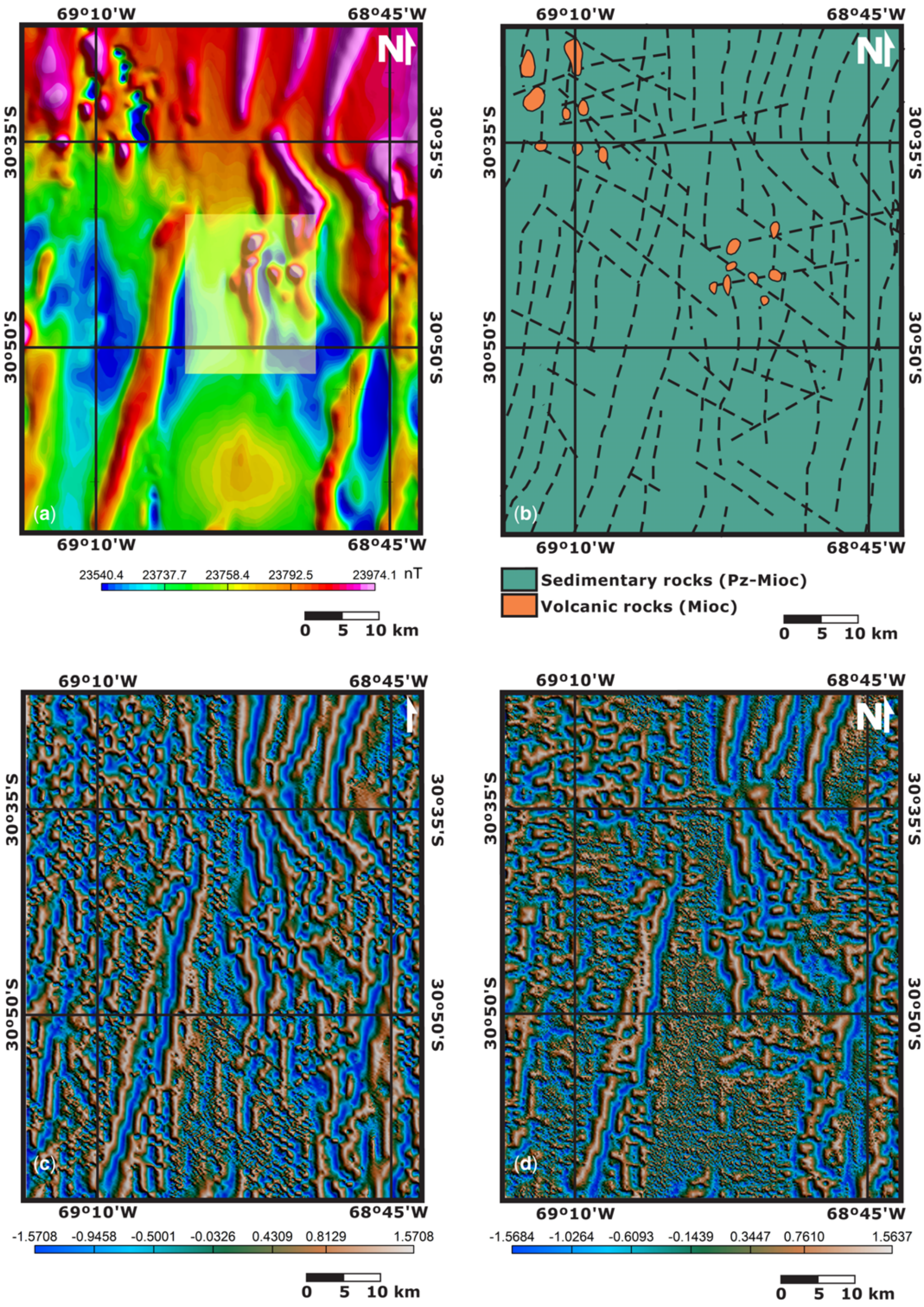

Fig. 7. (**a**) Map of magnetic anomaly reduced to pole. The study area (Fig. 2) is shown with a yellow rectangle. (**b**) Lithomagnetic domains and lineaments interpreted over the magnetic anomaly reduced to pole and first derivatives, respectively. (**c**) First horizontal derivative. (**d**) First vertical derivative.

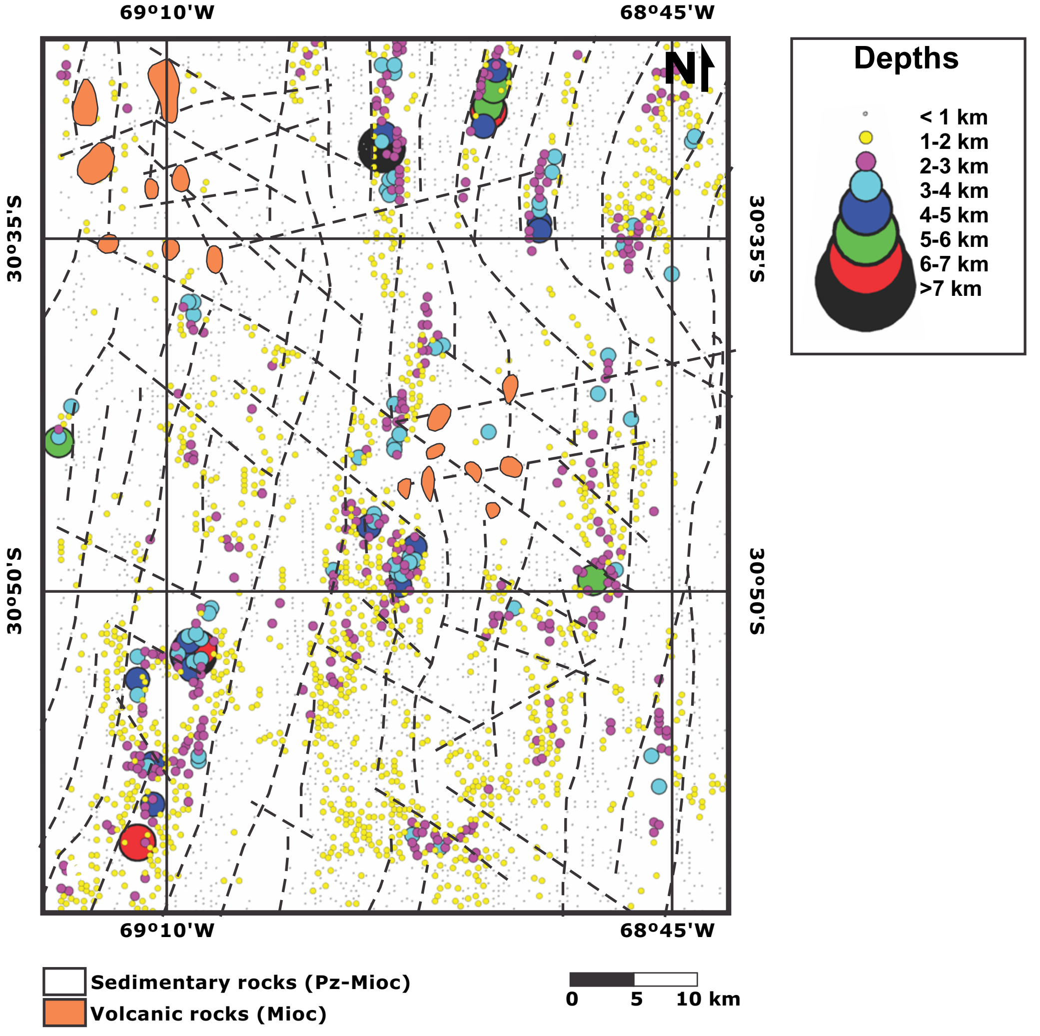

Fig. 8. Lithomagnetic domains and lineaments (modified from Fig. 7b) with estimated depths obtained from source parameter imaging (dots).

NW cross-strike structures in three different areas (Fig. 3b) already recognized by Ré *et al.* (2001). They represent steeply dipping brittle–ductile shear zones that develop at different scales (see 'Structure of the Hualilán area'). Both field relationships and regional observations show that ENE structures are subordinate to those of WNW.

Lithomagnetic domains and lineaments recognized in Figure 7b reveal the presence of two areas where oblique lineaments and Miocene igneous rocks are both concentrated. Both localities are linked by some major WNW lineaments, as shown in Figure 7b, and are aligned in a WNW–NW direction. These results are in agreement with structural data and confirm the existence of cross-strike structures below the Holocene deposits in the Pampa de Hualilán, supporting proposals from Oriolo (2012) and Oriolo *et al.* (2012) based on geomorphological studies.

SPI solutions are mostly aligned with NNE lineaments (Fig. 8). Therefore, they are interpreted to represent NNE Andean thrusts. Cross-strike structures are only locally defined by alignments of SPI solutions, although WNW and ENE lineaments give rise to strong NNE along-strike segmentation in their grouping and depths. Differences between first derivatives (Fig. 7b) and the SPI method (Fig. 8) regarding the presence of cross-strike structures can be explained by their orientation. They are mostly subvertical structures that cannot be detected easily by the SPI method because of their steep dips (Fig. 4a).

Areas with scarce SPI solutions could be the result of the presence of a sedimentary cover. However, they could also be explained by the presence of several cross-strike structures (Figs 2 & 7b) and the small dimensions of Miocene igneous bodies, which are also well grouped, because these could give rise to interference patterns that would overcome the method resolution.

The geological, structural and geophysical data listed above led to the definition of the presence of WNW and subordinated ENE cross-strike structures in the Central Andes. These may have controlled the emplacement of Miocene magmatism migrating into the foreland due to the flattening of the slab, as field relationships and structural observations have shown. Magmatism could migrate along WNW cross-strike structures whereas it could be emplaced where WNW and ENE features are both present. Despite being dominantly strike-slip structures, minor normal dip-slip kinematic analysis would give rise to the local extension required for volcanic output (Acocella & Funiciello 2010). Moreover, approximately east–west-trending mineralized veins genetically related to Neogene magmatism in the Hualilán area were described by Pelichotti (1976) as supporting local extension. WNW-trending half-graben described by Costa & Cortés (1993) and the WNW transtensional volcanic belt defined by Japas *et al.* (2010) in the Sierras Pampeanas (Fig. 1a) also support the kinematics presented herein.

Cross-strike structures in the study area indicate the presence of the Hualilán Belt (Oriolo *et al.* 2011; Oriolo 2012), which is equivalent to the Talacasto lineament previously defined by Ré *et al.* (2001) and which represents the structural control of the Miocene Central Volcanic Belt of the Precordillera (Oriolo 2012). Based on similar relationships (Fig. 3b), the presence is also proposed, of two other equivalent WNW sinistral transtensional belts controlling Miocene volcanic emplacement in the Precordillera that could be coincident with domain I, sectors A and C (Fig. 3b). This is more evident at 29°45′S where WNW to NW structures and magmatic rocks were documented by Chernicoff & Nash (2002).

The brittle–ductile nature of cross-strike structures could be explained as the result of the Rebinder effect (Karpenko 1974) and hydraulic fracturing that could give rise to strain softening due to the presence of magmatic fluids and thermal activation. However, Hindle & Vietor (2005) suggest that deformation of cross-strike structures is distributed over wide zones made up of minor structures but they do not link these features to the presence of magmatism.

Temporal and kinematic evolution of cross-strike structures

Field data suggest that magmatism and the main tectonic activity of WNW to ENE structures have taken place after the main uplift of the Andean thrusts as Pelichotti (1976) and Oriolo (2012) had previously suggested. Ages between 9 and 6 Ma obtained from other volcanic and subvolcanic rocks from the Precordillera (Kay & Mpodozis 2002) are consistent with this proposal. This supports the relationship between oblique structures and magmatism already mentioned (see ‘Discussion’).

The regional variation of the magnetic field from a NNE to SSW direction and cross-cutting relationships with those magnetic anomalies interpreted as thrusts (Fig. 7b) suggest a probable ‘inherited’ nature of the highly oblique lineaments. Analogue modelling and gravimetric data considered by Oriolo (2012) and Oriolo *et al.* (2012) have also supported this hypothesis. Likewise, analogue models from these authors have demonstrated that cross-strike structures do not develop unless they represent pre-existing crustal fabrics but they reactivate after the main shortening in orogenic along-strike structures has occurred. According to results obtained by the SPI method (see ‘Source parameter imaging (SPI)’), these structures must be located mostly at depths up to 5 km so they can be developed in a pre-Miocene basement. Moreover, WNW structures in the Hualilán area could be associated with the Pie de Palo Norte lineament, located between the Sierra de Pie de Palo and the Eastern Precordillera (Fig. 1b). Using seismic data, Zapata (1998) has described the lineament as a steeply dipping sinistral strike-slip flower structure in the Bermejo valley that causes left-lateral offsets of Tertiary units in the Eastern Precordillera (Milana 1990).

Siame *et al.* (2005) have provided kinematic data that demonstrate a regional west–WNW shortening for the Precordillera that gives rise to almost north-striking folds and thrusts that have developed since Late Miocene times. On the other hand, kinematic results obtained in this study (see ‘Kinematic Analysis’) reveal that cross-strike structures show a strong component of strike-slip displacements. Siame *et al.* (2005) have also proposed a clockwise reorientation of kinematic axes in the Precordillera that could have begun between 5 and 2.5 Ma; their proposal is also supported by data obtained in this work (see ‘Kinematic Analysis’). This reorientation can be restricted to the Late Miocene–Pliocene? for the study area, as the temporal relationship between magmatism (9 to 6 Ma according to Kay & Mpodozis 2002) and its structural controls suggests (activation of cross-strike structures since *c.* 9 Ma post-dating the main tectonic activity of thrusts; see Oriolo 2012 and references therein). Therefore, kinematics showing minor extension associated with cross-strike structures obtained in Hualilán are local and resulted from the reactivation of ancient structures during an Andean transpressional regime in the Precordillera (Siame *et al.* 2005). These results are significantly different from regional ones but they are consistent with the regional Andean deformation. The similar reorientation pattern between both local and regional kinematic axes (Siame *et al.* 2005) also supports this idea.

Conclusions

The data presented in this paper have led to an increased understanding of the kinematics and development of cross-strike structures in the study area and its regional framework:

(1) The presence of cross-strike structures in the Precordillera is confirmed. They represent WNW brittle–ductile belts with sinistral strike-slip displacements and are probably the result of reactivation of pre-existing crustal fabrics during the Andean orogeny. Particularly, the Hualilán Transtensional Belt is defined for the study area.

(2) Cross-strike structures represent the main structural control in the emplacement of Miocene magmatism migrating into the foreland due to the Andean flat-slab subduction.

(3) Kinematics of cross-strike structures show mostly strike-slip displacements in spite of approximately north-striking thrusting and folding observed at regional scale, though they are all consistent with regional Andean transpressional deformation. Moreover, the regional clockwise reorientation of kinematic axes has also affected the local pattern of deformation since Late Miocene–Pliocene? times.

The authors wish to thank projects PIP CONICET 11420100100334 (M. S. Japas), PICT 2010-1441 and UBACyT 20020100100855 (E. O. Cristallini). J. Cortés, H. Vizán and J. Sellés-Martínez are acknowledged for previous discussions related to this work. We thank the editors and L. Giambiagi and a second anonymous reviewer for helpful comments and corrections that enabled us to improve this manuscript. We also thank R. Allmendinger and R. Holcombe for free access to software.

References

Acocella, V. & Funiciello, F. 2010. Kinematic setting and structural control of arc volcanism. *Earth and Planetary Science Letters*, **289**, 43–53.

Allmendinger, R. W., Figueroa, D., Snyder, D., Beer, J., Mpodozis, C. & Isacks, B. L. 1990. Foreland shortening and crustal balancing in the Andes at 30°S latitude. *Tectonics*, **9**, 789–809.

Allmendinger, R. W., Cardozo, N. & Fisher, D. 2012. *Structural Geology Algorithms: Vectors and Tensors in Structural Geology*. Cambridge University Press, Cambridge.

Baldis, B. & Vaca, A. 1985. Megafracturas relacionadas con el sistema cordillerano. *Primeras Jornadas sobre Geología de Precordillera, Actas*, **1**, 204–208.

Baranov, V. 1957. A new method for interpretation of aeromagnetic maps: pseudo-gravimetric anomalies. *Geophysics*, **22**, 359–383.

Bastias, H. 1985. *Fallamiento cuaternario en la región sismotectonica de Precordillera*. PhD thesis, Universidad Nacional de San Juan.

Bastías, H., Weidmann, N. & Pérez, M. 1984. Dos zonas de fallamiento plio–cuaternario en la Precordillera de San Juan. *IX Congreso Geológico Argentino, Actas*, **2**, 329–341.

Blakely, R. J. 1995. *Potential Theory in Gravity and Magnetic Applications*. Cambridge University Press, Cambridge.

Blakely, R. J. & Simpson, R. W. 1986. Approximating edges of source bodies from magnetic or gravity anomalies. *Geophysics*, **51**, 1494–1498.

Brown, M. & Solar, G. S. 1999. The mechanism of ascent and emplacement of granite magma during transpression: a syntectonic granite paradigm. *Tectonophysics*, **312**, 1–33.

Cahill, T. & Isacks, B. L. 1992. Seismicity and the shape of the subducted Nazca plate. *Journal of Geophysical Research*, **97**, 17503–17529.

Chernicoff, C. J. & Nash, C. R. 2002. Geological interpretation of Landsat TM imagery and aeromagnetic survey data, northern Precordillera region, Argentina. *Journal of South American Earth Sciences*, **14**, 813–820.

Chernicoff, C. J., Richards, J. P. & Zappettini, E. O. 2002. Crustal lineament control on magmatism and mineralization in northwestern Argentina: geological, geophysical, and remote sensing evidence. *Ore Geology Reviews*, **21**, 127–155.

Costa, C. & Cortés, J. M. 1993. Tectónica extensional en el extremo sur de la sierra de San Luis. *XII Congreso Geológico Argentino, Actas*, **3**, 113–118.

Cristallini, E. O. & Ramos, V. A. 2000. Thick-skinned and thin-skinned thrusting in La Ramada fold and thrust belt: crustal evolution of the High Andes of San Juan, Argentina (32° SL). *Tectonophysics*, **317**, 205–235.

De Saint Blanquat, M. & Tikoff, B. 1997. Development of magmatic to solid-state fabrics during syntectonic emplacement of the Mono Creek Granite, Sierra Nevada Batholith. *In*: Bouchez, J. L., Hutton, D. & Stephens, D. E. (eds) *Granite: From Segregation of Melts to Emplacement Fabrics*. Kluwer Academic, Dordrecht, 231–252.

De Saint Blanquat, M., Tikoff, B., Teyssier, C. & Vigneresse, J. L. 1998. Transpressional kinematics and magmatic arcs. *In*: Holdsworth, R. E., Strachan, R. A. & Dewey, J. F. (eds) *Continental Transpressional and Transtensional Tectonics*.

Geological Society, London, Special Publications, **135**, 327–340.

Gansser, A. 1973. Facts and theories on the Andes: Twenty-sixth William Smith Lecture. *Journal of the Geological Society, London*, **129**, 93–131.

Gómez Rivarola, L. 2007. *Descripción e interpretación de las rocas volcánicas, volcaniclásticas y facies sedimentarias asociadas en la región de Cerro Negro de Iglesia, Precordillera Occidental, Provincia de San Juan*. Trabajo Final de Licenciatura, Universidad de Buenos Aires.

Gutscher, M., Maury, R., Eissen, J. P. & Bourdon, E. 2000. Can slab melting be caused by flat subduction? *Geology*, **28**, 535–538.

Heredia, N., Rodríguez Fernández, L. R., Gallastegui, G., Busquets, P. & Colombo, P. 2002. Geological setting of the Argentine Frontal Cordillera in the flat slab segment (30°00′–31°30′S latitude). *Journal of South American Earth Sciences*, **15**, 79–99.

Hindle, D. & Vietor, T. 2005. 3D strain modeling of tear fault analogues. Abstract #S53A-1091, presented at the *American Geophysical Union, Fall Meeting 2005*.

Holcombe, R. 2011. GEOrient 9.5.0. Stereographic Projections and Rose Diagrams Plots. http://www.holcombecoughlinoliver.com/holcombe/.

Hudnut, K., Seeber, L., Rockwell, T., Goodmacher, J., Klinger, R., Lindvall, S. & Mcelwain, R. 1989. Surface ruptures on cross-faults in the 24 November 1987 Superstition Hills, California, earthquake sequence. *Bulletin of the Seismological Society of America*, **79**, 282–296.

Japas, M. S. 1998. Aporte del análisis de fábrica deformacional al estudio de la faja orogénica andina. Homenaje al Dr. Arturo J. Amos. *Revista de la Asociación Geológica Argentina*, **53**, 15.

Japas, M. S. & Ré, G. H. 2005. Geodynamic impact of arrival and subduction of oblique aseismic ridges. In: *VI International Symposium on Andean Geodynamics, abstracts*, 408–410.

Japas, M. S. & Ré, G. H. 2012. Neogene tectonic block rotations and margin curvature at the Pampean flat slab segment (28°–33° SL, Argentina). *Geoacta*, **37**, 1–4.

Japas, M. S., Ré, G. H. & Barredo, S. P. 2002*a*. Lineamientos andinos oblicuos (entre 22° y 33° S): definidos a partir de fábricas tectónicas. I. Fábrica deformacional y de sismicidad. *XV Congreso Geológico Argentino, Actas*, **I**, 326–331.

Japas, M. S., Ré, G. H. & Barredo, S. P. 2002*b*. Lineamientos andinos oblicuos (entre 22° y 33° S) definidos a partir de fábricas tectónicas. III. Modelo cinemático. *XV Congreso Geológico Argentino, Actas*, **I**, 340–343.

Japas, M. S., Cortés, J. M. & Pasini, M. 2008. Tectónica extensional triásica en el sector norte de la cuenca Cuyana: primeros datos cinemáticos. *Revista de la Asociación Geológica Argentina*, **63**, 213–222.

Japas, M. S., Urbina, N. E. & Sruoga, P. 2010. Control estructural en el emplazamiento del volcanismo y mineralizaciones neógenas, distrito Cañada Honda, San Luis. *Revista de la Asociación Geológica Argentina*, **67**, 494–506.

Japas, M. S., Sruoga, P., Kleiman, L. E., Gayone, M. R., Maloberti, A. & Comito, O. 2011*a*. Cinemática de la extensión jurásica vinculada a la provincia silícea Chon Aike, Santa Cruz, Argentina. *XVIII Congreso Geológico Argentino, Actas*, 97–98.

Japas, M. S., Urbina, N. E., Sruoga, P. & Gallard, M. C. 2011*b*. La Carolina pull-apart in western Tertiary Volcanic Belt, Pampean Flat Slab (33°S), Argentina. *XXII Lateinamerika Kolloquium*.

Japas, M. S., Sruoga, P., Kleiman, L. E., Gayone, M. R., Maloberti, A. & Comito, O. 2013. Cinemática de la extensión jurásica vinculada a la provincia silícea Chon Aike, Santa Cruz, Argentina. *Revista de la Asociación Geológica Argentina*, **70**, 16–30.

Johnson, C. A,, Sattar, M. A., Rosell, R., Al–Shekaili, F., Al–Zaabi, N. & Gombos, A. 2002. Structure and regional context of onshore Fields in Abu Dhabi, UAE. *Society of Petroleum Engineers, Conference Paper*, http://dx.doi.org/10.2118/78488-MS.

Karpenko, G. V. 1974. The 45th anniversary of the Rebinder effect. *Materials Science*, **10**, 3–4.

Kay, S. M. & Abbruzzi, J. M. 1996. Magmatic evidence for Neogene lithospheric evolution of the central Andean 'flat-slab' between 30°S and 32°S. *Tectonophysics*, **259**, 15–28.

Kay, S. M. & Mpodozis, C. 2002. Magmatism as a probe to the Neogene shallowing of the Nazca plate beneath the modern Chilean flat-slab. *Journal of South American Earth Sciences*, **15**, 39–57.

Lara, L. E., Lavenu, A., Cembrano, J. & Rodríguez, C. 2006. Structural controls of volcanism in transversal chains: resheared faults and neotectonics in the Cordón Caulle–Puyehue area (40.5°S), Southern Andes. *Journal of Volcanology and Geothermal Research*, **158**, 70–86.

Leveratto, M. A. 1976. Edad de intrusivos cenozoicos en la Precordillera de San Juan y su implicancia estratigráfica. *Revista de la Asociación Geológica Argentina*, **31**, 53–58.

Limarino, C. O., Fauqué, L. A., Cardó, R., Gagliardo, M. L. & Escosteguy, L. 2002. La faja volcánica miocena de la Precordillera septentrional. *Revista de la Asociación Geológica Argentina*, **57**, 289–304.

Lin, J., Stein, R. S., Meghraoui, R., Toda, S., Ayadi, A., Dorbath, C. & Belabbes, S. 2011. Stress transfer among en echelon and opposing thrusts and tear faults: triggering caused by the 2003 Mw = 6.9 Zemmouri, Algeria, earthquake. *Journal of Geophysical Research*, **116**, B03305, http://dx.doi.org/10.1029/2010JB007654.

Logan, M. A. 2000. Mineralogy and geochemistry of the Argentina. *Ore Geology Reviews*, **17**, 113–138.

Marrett, R. A. & Allmendinger, R. W. 1990. Kinematic analysis of fault-slip data. *Journal of Structural Geology*, **12**, 973–986.

Milana, J. P. 1990. *Sedimentología y magnetoestratigrafía de formaciones cenozoicas en el área de Mogna, y su incersión en el marco tectosedimentario de la Precordillera Oriental*. PhD thesis, Universidad Nacional de San Juan.

Mueller, K. & Talling, P. 1997. Geomorphic evidence of tear faults accommodating lateral propagation of an active fault-bend fold, Wheeler Ridge, California. *Journal of Structural Geology*, **19**, 397–411.

Nabighian, M. N. 1972. The analytical signal of two-dimensional bodies with polygonal cross-section: its properties and use for automated interpretations. *Geophysics*, **37**, 780–786.

Nabighian, M. N. 1974. Additional comments on the analytical signal of two-dimensional bodies with polygonal cross-section. *Geophysics*, **39**, 85–92.

Nabighian, M. N. 1984. Towards a three-dimensional automatic interpretation of potential field data via generalized Hilbert transforms: fundamental relations. *Geophysics*, **49**, 780–786.

Oriolo, S. 2012. *Análisis de la deformación en la región de Hualilán, Precordillera de San Juan*. Trabajo Final de Licenciatura, Universidad de Buenos Aires.

Oriolo, S., Japas, M. S. & Cristallini, E. O. 2011. Transtensional megashear zones in the Central Andes: the Hualilán Belt. *Deformation Mechanisms, Rheology and Tectonics Conference Proceedings*, 95.

Oriolo, S., Cristallini, E. O. & Japas, M. S. 2012. Modelos análogos aplicados a sistemas transpresivos y transtensivos. Jornada Abierta del Instituto de Geociencias IGEBA, Tectónica de Desplazamiento de Rumbo, actas, **12**.

Pelichotti, R. 1976. *Estudio geológico–económico y proyecto de exploración del Distrito Minero Gualilán, Dpto. Ullúm, Pcia. de San Juan*. Servicio Minero Nacional, Plan San Juan.

Petrinovic, I., Riller, U. & Brod, J. A. 2005. The Negra Muerta Volcanic Complex, southern Central Andes: geochemical characteristics and magmatic evolution of an episodically active volcanic centre. *Journal of Volcanology and Geothermal Research*, **144**, 295–320.

Petrinovic, I., Martí, J., Aguirre–Díaz, G. J., Guzmán, S., Geyer, A. & Salado Paz, N. 2010. The Cerro Aguas Calientes caldera, NW Argentina: an example of a tectonically controlled, polygenetic, collapse caldera, and its regional significance. *Journal of Volcanology and Geothermal Research*, **194**, 15–26.

Pilger, R. H. 1981. Plate reconstructions, aseismic ridges, and low angle subduction beneath the Andes. *Geological Society of America Bulletin*, **92**, 448–456.

Pizzi, A. & Galadini, F. 2009. Pre-existing cross-structures and active fault segmentation in the northern-central Apennines (Italy). *Tectonophysics*, **476**, 304–319.

Pohn, H. A. 2000. *Lateral ramps in the folded Apalaches and in overthrust belts worldwide – a fundamental element of thrust-belt architecture*. US Geological Survey Bulletin, **2163**.

Ragona, D., Anselmi, G., González, P. & Vujovich, G. 1995. *Mapa Geológico de la Provincia de San Juan. Escala 1:500 000*. SEGEMAR, Buenos Aires.

Ramos, V. A., Cristallini, E. O. & Pérez, D. J. 2002. The Pampean flat-slab of the Central Andes. *Journal of South American Earth Sciences*, **15**, 59–78.

Ramsay, J. G. & Huber, M. I. 1987. *The Techniques of Modern Structural Geology (2: Fold and Fractures)*. Academic Press, London.

Ré, G. H. & Japas, M. S. 2004. Andean oblique megashear zones: paleomagnetism contribution. *GSA Abstract with Programs*, **36**, Abstract No. 79033.

Ré, G. H., Japas, M. S. & Barredo, S. P. 2000. Análisis de fábrica deformacional (AFD): el concepto fractal cualitativo aplicado a la definición de lineamientos cinemáticos neógenos en el noroeste argentino. *X Reunión sobre Microtectónica, Resúmenes*, 12.

Ré, G. H., Japas, M. S. & Barredo, S. P. 2001. Análisis de fábrica deformacional (AFD): el concepto fractal cualitativo aplicado a la definición de lineamientos cinemáticos neógenos en el noroeste argentino. *Revista de la Asociación Geológica Argentina Serie D*, Publicación Especial, **5**, 75–82.

Riller, U., Petrinovic, I., Ramelow, J., Strecker, M. & Oncken, O. 2001. Late Cenozoic tectonism, collapse caldera and plateau formation in the central Andes. *Earth and Planetary Science Letters*, **188**, 299–311.

Roest, W. R., Verhoef, J. & Pilkington, M. 1992. Magnetic interpretation using the 3–D analytical signal. *Geophysics*, **51**, 116–125.

Romeo, I., Capote, R., Tejero, R., Lunar, R. & Quesada, C. 2006. Magma emplacement in transpression: the Santa Olalla Igneous Complex (Ossa–Morena Zone, SW Iberia). *Journal of Structural Geology*, **28**, 1821–1834.

Rossello, E. A., Mozetic, M. E., Cobbold, P. R., de Urreiztieta, M. & Gapais, D. 1996. El espolón Umango-Maz y la conjugación sintaxial de los Lineamientos Tucumán y Valle Fértil (La Rioja, Argentina). *XIII Congreso Geológico Argentino y III Congreso de Exploración de Hidrocarburos, actas*, **2**, 187–194.

Saha, T., Chowdhury, B. K., Chakraborthy, D., Prusty, S. K., Khatri, B. L. & Reddy, G. V. 2006. Understanding structural configuration on the basis of 3D seismic attributes in Dhansiri Valley, Assam. *Geohorizons*, **2**, 28–31.

Salfity, J. A. 1985. Lineamientos transversales al rumbo andino en el Noroeste Argentino. *IV Congreso Geológico Chileno, Actas*, **2**, 119–137.

Sanderson, D. J. & Marchini, W. R. D. 1984. Transpression. *Journal of Structural Geology*, **6**, 449–458.

Siame, L. L., Bellier, O., Sebrier, M. & Araujo, M. 2005. Deformation partitioning in flat subduction setting: case of the Andean foreland of western Argentina (28°S–33°S). *Tectonics*, **24**, http://dx.doi.org/10.1029/2005TC001787.

Sruoga, P. & Urbina, N. E. 2008. Volcanismo en ambiente de flat-slab: Cañada Honda, Sierras Pampeanas de San Luis (32° 50′S, 66° 00′O). *XVII Congreso Geológico Argentino, Actas*, **1**, 238–239.

Sruoga, P., Urbina, N. E. & Malvicini, L. 1996. El Volcanismo Terciario y los depósitos hidrotermales (Au,Cu) asociados en La Carolina y Diente Verde, San Luis, Argentina. *XIII Congreso Geológico Argentino, Actas*, **3**, 89–100.

Tavarnelli, E., Butler, R. W. H., Decandia, F. A., Calamita, F., Grasso, M., Alvarez, W. & Renda, P. 2004. Implications of fault reactivation and structural inheritance in the Cenozoic tectonic evolution of Italy. *In*: Crescenti, U., D'Offizi, S., Merlini, S. & Sacchi, R. (eds) *The Geology of Italy*. Societa Geologica Italiana, Rome, Special Volume, 209–222.

Twiss, R. J. & Moore, E. M. 1992. *Structural Geology*. Freeman & Co, New York.

Urbina, N. E. & Sruoga, P. 2009. La faja metalogenética de San Luis: mineralización y geocronología en el contexto metalogenético regional. *Revista de la Asociación Geológica Argentina*, **64**, 635–645.

Urbina, N. E., Sruoga, P. & Malvicini, L. 1995. El volcanismo Mioceno y la mineralización aurífera asociada en La Carolina y Diente Verde, provincia de San Luis, Argentina. *IX Congreso Latinoamericano de Geología, Actas*, 1–13.

Urbina, N. E., Sruoga, P. & Malvicini, L. 1997. Late tertiary gold-bearing volcanic belt in the Sierras Pampeanas of San Luis, Argentina. *International Geology Review*, **39**, 287–306.

Urreiztieta, M. 1996. *Tectonique Néogène et basins transpressifs en bordure méridionale de l'Altiplano-Puna (27°S), Nord-Ouest argentin*. Memoires, Geosciences Rennes. PhD thesis, Université de Rennes I.

Van Gool, J. A. M. & Piazolo, S. 2006. Presentation and interpretation of structural data from the Nagssugtokidian orogen using a GIS platform: general trends and features. *Geological Survey of Denmark and Greenland Bulletin*, **11**, 125–144.

Wheeler, R. L. 1980. Cross-strike structural discontinuities: possible exploration tool for natural gas in Appalachian overthrust belt. *American Association of Petroleum Geologists Bulletin*, **64**, 2166–2178.

Žák, J., Holub, F. V. & Verner, K. 2005. Tectonic evolution of a continental magmatic arc from transpression in the upper crust to exhumation of mid-crustal orogenic root recorded by episodically emplaced plutons: the Central Bohemian Plutonic Complex (Bohemian Massif). *International Journal of Earth Sciences*, **95**, 385–400.

Zapata, T. R. 1998. Crustal structure of the Andean thrust front at 30°S latitude from shallow and deep seismic reflection profiles, Argentina. *Journal of South American Earth Sciences*, **11**, 131–151.